Journal of Sound and Vibration (2001) **242**(1), 69–83
doi:10.1006/jsvi.2000.3363, available online at http://www.idealibrary.com on IDEAL®

RESPONSE OF MODULATED DOUBLET MODES TO TRAVELLING WAVE EXCITATION

J. Y. Chang and J. A. Wickert

Department of Mechanical Engineering, Carnegie Mellon University, Pittsburgh, PA 15213-3890, *USA*

(*Received* 30 *May* 2000, *and in final form* 11 *September* 2000)

The forced vibration of a rotationally periodic structure when subjected to travelling wave excitation is discussed, with emphasis placed on the steady-state response of doublet modes having either repeated or split frequencies. Such vibration modes have spatially modulated shapes defined by (1) the number of nodal diameters present in the limiting case of axisymmetry, and (2) certain additional Fourier harmonics which contaminate and distort their appearances. The natural frequency and mode structure of a model periodic structure is discussed in the context of an otherwise axisymmetric disk having evenly spaced, sector-shaped, line distributions of stiffness and inertia. Through perturbation analysis, the contamination wavenumbers present in a doublet having repeated frequency are shown to comprise two subsets, the members of which have sine and cosine coefficients of the same, or of differing, signs for each wavenumber in the mode shape's Fourier expansion. The structure of the wavenumber content is explored further with respect to the response of repeated and split doublets to a harmonic travelling wave excitation. The individual Fourier components comprising a modulated doublet can respond and propagate in the same direction as the excitation, or opposite to it, depending on the wavenumber of the excitation and the subset to which the contamination wavenumber belongs. The response of the split frequency doublets and the circumstances under which travelling or standing wave responses, or a blend of the two, can occur in the structure's reference frame are also examined in the context of the model periodic structure. The qualitative character of the response, the forward or backward propagation direction of each mode's constituent wavenumber components, and the phase speeds of those components are discussed in illustrative case studies.

1. INTRODUCTION

Turbine assemblies, fans, pumps, gears, automotive and aircraft braking systems, and the clamping collars used in computer disk drives are examples of rotationally periodic structures. This class of system is defined by having a regular geometry that is preserved following rotation of the entire structure through a certain angle. When such features as the blades in a radial flow impeller, the cooling fins in a brake rotor, or the bolts in a clamping collar are incorporated in an otherwise axisymmetric shell- or disk-like structural model, the natural frequencies, vibration modes, and response characteristics each shift and change. The forced response of rotationally periodic structures when they are subjected to harmonic travelling wave excitation, and in particular, the behavior of their repeated and split frequency doublet vibration modes, form the subject of this investigation. Such forcing functions are measured in the structure's frame of reference, with some examples including the pressure field established by upstream stator vanes on a bladed disk assembly, normal loading of a brake pad on a rotor, and the interaction of a rigid magnetic disk with its recording head and suspension assembly.

0022-460X/01/160069 + 15 $35.00/0

In the absence of periodic features, the vibration modes of an axisymmetric shell- or disk-like structure are classified as being either doublets (in which case two linearly independent sine- and cosine-oriented vibration modes of common frequency exist) or as singlets (where the frequency is instead an isolated root of a characteristic equation, and the vibration mode itself is axisymmetric). Those two classes of modes are further categorized according to the numbers m and n of nodal circles and diameters, respectively, where $n = 0$ for all singlets.

As periodic features are incrementally added to the structure, the natural frequencies of certain doublet modes split into distinct values, but the frequencies of all other doublets remain repeated. Further, the mode shapes of each doublet class—those repeated and those split in frequency—become contaminated with by the presence of additional Fourier harmonics beyond the base wavenumber n. As they superpose on the disk's underlying nodal diameter pattern, those contamination harmonics can produce a distorted, spatially modulated appearance [1].

Because of their technological importance and interesting mechanics, a rich literature exists in the field of rotationally periodic systems. Model structures used in examining the natural frequencies and mode shapes include a ring with point stiffness supports, distributed evenly in the circumferential direction, bolted plate and flange assemblies, and radial or axial flow turbine components. The early studies by Thomas [2, 3] were based on finite element methods in which substructure-level stiffness and mass matrices were assembled and used to describe the composite structure's dynamics. Allaei *et al.* [4] used the receptance method to characterize the in-plane mode shapes of a ring having radially oriented spring attachments. Frequency splitting in periodic, yet almost axisymmetric, structures has been analyzed with a view towards developing criteria to predict when the otherwise repeated frequencies of the nodal diameter modes split into different values [5–9]. Ewins and Imregun [10] combined the use of finite element models and laboratory measurements to examine frequency shifts and mode shape distortion occurring in packeted bladed disks. Tomioka *et al.* [11] similarly examined coupled disk–blade systems through a Ritz discretization approach.

Primarily modal expansion techniques have been used in treating the forced response problem. When an axisymmetric structure is subjected to a harmonic travelling wave excitation, a particular nodal diameter mode is excited, only when the excitation's wavenumber is commensurate with the mode's number of nodal diameters. Accordingly, near resonance of a doublet having repeated frequency, an axisymmetric structure responds in a travelling wave, where the response and excitation have common wavenumbers and phase speeds. Several analytical and experimental studies [12–15] discuss forward and backward travelling response waves in that regard. Campbell diagrams, for instance, are often used to explain resonant conditions in terms of commensurate excitation and natural frequencies as a function of rotation speed and excitation order [16]. The standing and travelling wave responses of bladed disk systems have been examined in references [17–20], among others, in which the dependencies of the response and resonance conditions on the number of blades, the number of nodal diameters, and the wavenumber of the excitation were examined.

In what follows, the response of a model periodic structure as it is subjected to a travelling excitation source is examined through a hybrid perturbation and modal expansion approach. The structure of the wavenumber content in the repeated and split frequency doublets is discussed in order to classify the contamination wavenumbers into two subsets according to the signs taken by the sine and cosine coefficients in the mode shapes' Fourier representations. The components comprising the forced response of a repeated frequency doublet are shown to be able to propagate in the same direction as the excitation, or

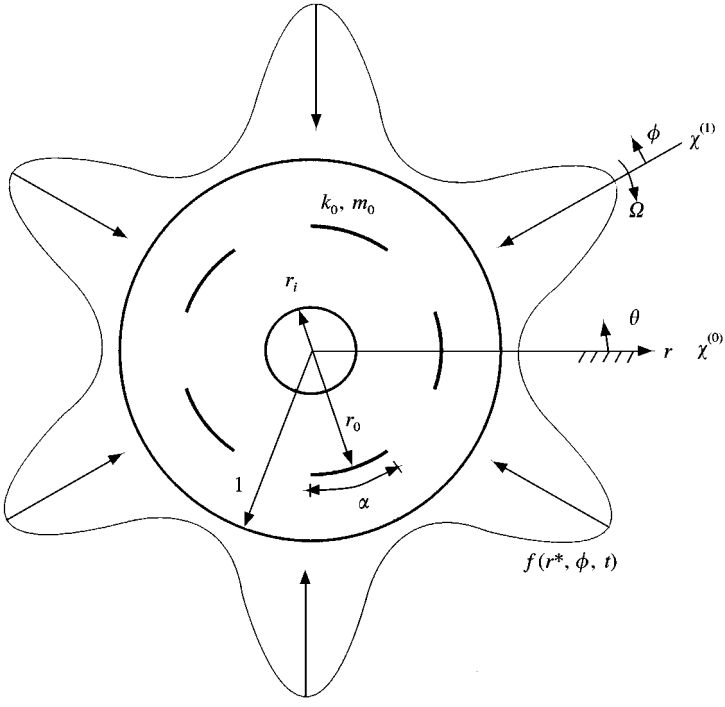

Figure 1. Schematic of a rotationally periodic structure comprising an otherwise axisymmetric disk having $NF = 5$ sector-shaped, evenly distributed, stiffness and inertia features at common radii r_0. The structure is subjected to the travelling wave excitation f which propagates clockwise at speed Ω.

opposite to it, depending on whether particular algebraic relationships are satisfied by the wavenumbers of the excitation and the contamination component. The circumstances under which travelling and standing wave response of the split frequency doublets, or a blend of the two, which can occur in the structure's reference frame are then examined in the context of a model periodic structure.

2. FREQUENCY AND MODE STRUCTURE

While the present focus lies on the forced response of doublet modes having wavenumber contamination, certain aspects of the free vibration problem are first reviewed and expanded upon. In particular, a certain relationship exists among the Fourier cosine A_k and sine B_k coefficients for each harmonic k present in a contaminated doublet, and that relationship has interesting forced-response implications.

In Figure 1, the thin, clamped–free, annular disk has NF identical, sector-shaped, line distributions of stiffness and inertia located at the common radial position r_0. This structure is stationary in the inertial reference frame $\chi^{(0)}$, with origin $\theta = 0$ aligned along the center of a feature. The disk is subjected to the travelling wave excitation f, acting normal to the disk's plane, which appears stationary in the concentric system $\chi^{(1)}$. Frame $\chi^{(1)}$ rotates clockwise relative to $\chi^{(0)}$ at the dimensionless speed Ω, defined as the ratio of the physical rotation speed to $\tau^{-1} = \sqrt{E/(1-v^2)\rho a^2}$, where ρ is the disk's volumetric mass density, v and E are its Poisson ratio and modulus, respectively, and a is the outer radius. The governing equations are formulated in $\chi^{(0)}$ in dimensionless form, wherein the outer radius is taken as

the characteristic length, and τ is the characteristic time scale. The disk's geometry is specified by the ratio $r_i = b/a$ of inner and outer radii.

Free vibration is represented by the more general, symbolic, eigenvalue problem $KU_i = \lambda_i MU_i$, in which K and M are dimensionless, positive definite, and self-adjoint stiffness and mass operators. For the disk vibration problem at hand, the eigenvalue is defined as $\lambda_i = (a/h)^2\omega_i^2$, where the dimensionless ω_i is the physical circular natural frequency scaled to τ, and h is the disk's thickness. The index $i = 1, 2, \ldots,$ denotes either a singlet or doublet eigenpair. Expanded to first order, the perturbed stiffness $K = K^{(0)} + \varepsilon K^{(1)}$ and mass $M = M^{(0)} + \varepsilon M^{(1)}$ operators comprise the contributions $K^{(0)}$ and $M^{(0)}$ associated with the axisymmetric structure, and components $K^{(1)}$ and $M^{(1)}$ which represent the periodic features. The small dimensionless parameter $\varepsilon \ll 1$ scales the loss of axisymmetry.

For a classical plate, $K^{(0)} = \nabla^4\cdot$ and $M^{(0)} = I\cdot$, where $\nabla^4\cdot$ is the biharmonic operator in polar coordinates, $I\cdot$ denotes the identity operator, and the bullet symbol indicates the operand's location. The stiffness and inertia distributions are represented as NF-periodic, piecewise constant, functions in θ having the Fourier representation

$$K^{(1)} = \frac{k_0}{r}\,\delta(r - r_0)\left[\frac{\alpha NF}{2\pi} + \sum_{j=1}^{\infty}\frac{2}{j\pi}\sin\left(\frac{j\alpha NF}{2}\right)\cos(jNF\theta)\right]\cdot, \tag{1}$$

$$M^{(1)} = \frac{m_0}{r}\,\delta(r - r_0)\left[\frac{\alpha NF}{2\pi} + \sum_{j=1}^{\infty}\frac{2}{j\pi}\sin\left(\frac{j\alpha NF}{2}\right)\cos(jNF\theta)\right]\cdot, \tag{2}$$

where δ is the Dirac function, and $0 \leqslant \alpha \leqslant 2\pi/NF$ is the span angle of each feature. Both K and M are preserved following the rotation of the entire structure through angle $\Delta\theta = 2\pi/NF$. The dimensionless constants k_0 and m_0 describe the local intensities of the stiffness and inertia features, where k_0 is the ratio of physical stiffness per unit length to E, and m_0 is the inertia per unit length scaled by ρh^2.

Following standard notation, the perturbed eigensolution is denoted as $\{\lambda_i, U_i\}$, and the presumably known solution for the neighboring axisymmetric problem is $\{\lambda_i^{(0)}, U_i^{(0)}\}$. The eigensolution is expressed to first order as $\lambda_i \approx \lambda_i^{(0)} + \varepsilon\lambda_i^{(1)}$ and $U_i \approx U_i^{(0)} + \varepsilon U_i^{(1)}$. Each $U_i^{(1)}$ is further expanded as a linear combination of the orthonormalized eigenfunctions U_{mn} of the axisymmetric structure, following reference [21], where the double subscript identifies the number of nodal circles and diameters present. Because the U_{mn} each comprise only one harmonic at wavenumber n, their relative amplitudes when superposed to form $U_i^{(1)}$ provide the wavenumber content of the contaminated eigenfunction.

2.1. REPEATED DOUBLETS

The first-order corrections to the natural frequencies and mode shapes are determined through expressions involving the unperturbed frequencies and modes, and their projections onto one another as weighted by $K^{(1)}$ and $M^{(1)}$. For specified n, the natural frequencies of the two members in the corresponding doublet mode of the perturbed structure remain repeated whenever $2n \neq jNF$, for $j = 1, 2, \ldots$. Those perturbed eigenvalues are approximated to first order by

$$\lambda_c = \lambda_s \approx \lambda_{c,s}^{(0)} + \varepsilon\lambda_{c,s}^{(1)} = \lambda_{c,s}^{(0)} + \varepsilon(\langle K^{(1)}U_{c,s}^{(0)}, U_{c,s}^{(0)}\rangle - \lambda_{c,s}^{(0)}\langle M^{(1)}U_{c,s}^{(0)}, U_{c,s}^{(0)}\rangle) \tag{3}$$

$$= \lambda_{c,s}^{(0)} + \varepsilon\frac{\alpha NF}{2}(k_0 - \lambda_{c,s}^{(0)}m_0)R_{mn}^2(r_0), \tag{4}$$

where the subscripts S and C denote the sine and cosine components, and $\lambda_{s,c}^{(0)}$ is their common eigenvalue at $\varepsilon = 0$. These frequencies increase or decrease with ε depending on the relative magnitudes of k_0 and m_0.

Each mode shape is perturbed through the introduction of certain other eigenfunctions of the neighboring problem, which enrich the harmonic content of U_i. By orienting $\chi^{(0)}$ so as to bisect a feature, the perturbed sine (cosine) mode is represented to first order as a linear combination of only the sine-oriented (cosine-oriented) members of other doublets. With arbitrary initial orientation of $\chi^{(0)}$, or with features that are not precisely periodic, the eigenfunctions of a repeated frequency doublet in the neighboring problem must instead be chosen as particular linear combinations of the sine and cosine members in order to present a uniform expansion in ε. The two elements of a repeated **R** doublet become

$$U_{mnc}^{(R)} = R_{mn}(r)\cos(n\theta) + \varepsilon \sum_{k \in \mathscr{K}} A_k^{(R)}(r)\cos(k\theta), \tag{5}$$

$$U_{mns}^{(R)} = R_{mn}(r)\sin(n\theta) + \varepsilon \sum_{k \in \mathscr{K}} B_k^{(R)}(r)\sin(k\theta), \tag{6}$$

where the index i has been replaced by notation indicating the numbers of nodal diameters and circles in $U_i^{(0)}$, and the mode's S or C symmetry. The set $\mathscr{K}$ of contamination wavenumbers is defined as those k satisfying the criterion $|n \pm k| = NF, 2NF, 3NF, \ldots$ [1, 10, 11]. The modulated doublets of the periodic P structure having repeated or split natural frequencies are henceforth denoted as $P(m, n)$ and $P(m, n)SC$, respectively, while the singlet modes are labelled $P(m, 0)$. This notation is adopted in order to explicitly distinguish these modes, which have an underlying pattern of nodal circles and diameters, from their companions in an axisymmetric structure.

The contamination wavenumbers comprise two integer subsets, namely $\mathscr{K} = \mathscr{M} \cup \mathscr{P}$, in which $\mathscr{M} = \{k : |n - k| = jNF\}$ (minus) and $\mathscr{P} = \{k : n + k = jNF\}$ (plus), where $j = 1, 2, \ldots$. For a particular k, the distinction as to whether $k \in \mathscr{M}$ or $k \in \mathscr{P}$ has implication for the signs and magnitudes of the $A_k^{(R)}$ and $B_k^{(R)}$ in equations (5) and (6). For each $k \in \mathscr{M}$,

$$A_k^{(R)}(r) = B_k^{(R)}(r) = C_{mnk}(r)\left(\frac{NF}{n-k}\right)\sin\left(\frac{n-k}{2}\alpha\right), \tag{7}$$

where as for each $k \in \mathscr{P}$,

$$A_k^{(R)}(r) = -B_k^{(R)}(r) = C_{mnk}(r)\left(\frac{NF}{n+k}\right)\sin\left(\frac{n+k}{2}\alpha\right). \tag{8}$$

The radial dependance is expressed by

$$C_{mnk}(r) = \frac{k_0 - \lambda_{c,s}^{(0)} m_0}{\lambda_{c,s}^{(0)} - \lambda_l^{(0)}} R_{mn}(r_0) R_{mk}(r_0) R_{mk}(r), \tag{9}$$

where $\lambda_{s,c}^{(0)}$ and $\lambda_l^{(0)}$ are the eigenvalues in the neighboring problem of the n and k nodal diameter modes. In equations (5) and (6), the coefficients $R_{mn}(r)$ of the components at wavenumber n are identical. For each k, the coefficients of the cosine $U_{mnc}^{(R)}$ and sine $U_{mns}^{(R)}$ doublet members depend on the separation between $\lambda_{c,s}^{(0)}$ and $\lambda_l^{(0)}$, and on the subset $\mathscr{M}$ or $\mathscr{P}$. In particular, the distinction $A_k^{(R)} = B_k^{(R)}$ or $A_k^{(R)} = -B_k^{(R)}$ in equations (7) and (8) has implication for the direction in which each response component propagates when the structure is excited subsequently by a travelling wave. Coefficients $A_k^{(R)}$ and $B_k^{(R)}$ are also functions of the features' sector angle, and they vanish in the two subsets when $\alpha = 2\pi j/(n \pm k)\,(j = 1, 2, \ldots)$. By proper selection of α, it is possible to reduce contamination

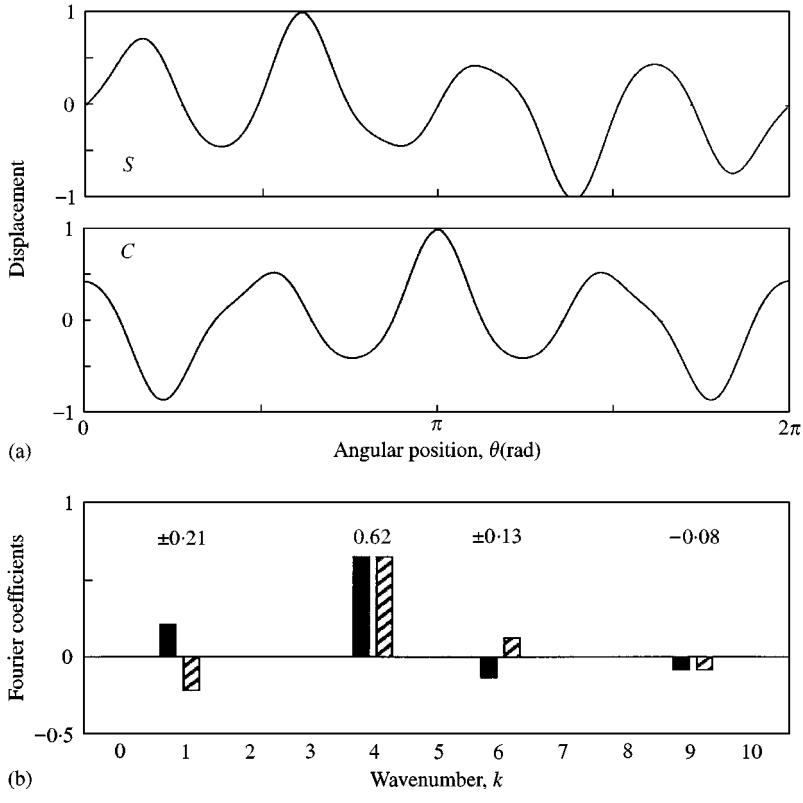

Figure 2. (a) Transverse displacements $U_{04S}^{(R)}$ and $U_{04C}^{(R)}$ at $r = 1$ of the $P(0, 4)$ doublet, and (b) Fourier coefficients R_{04}, $\varepsilon A_k^{(R)}$, ▨, and $\varepsilon B_k^{(R)}$, ■, at $k = 1$, 6 and 9.

at any particular wavenumber, or even eliminate it altogether,at least to first order. In equations (7) and (8), when the arguments $(n \pm k)\alpha/2$ are sufficiently small, $A_k^{(R)} = B_k^{(R)} = \alpha C_{mnk} NF/2$ for $k \in \mathscr{M}$, and $A_k^{(R)} = -B_k^{(R)} = \alpha C_{mnk} NF/2$ for $k \in \mathscr{P}$, so that the degree of modulation grows with the number of features and sector size.

Figures 2 and 3 depict results for the $P(0, 4)$ and $P(0, 6)$ doublets, which are asymptotic to the four and six nodal diameter doublets of the axisymmetric disk. In these examples, the disk's thickness is scaled to be 1% of its outer radius, $NF = 5$, $\alpha = \pi/10$, $k_0 = m_0 = 5$, $r_i = 0{\cdot}5$, $r_0 = 1$, and $\varepsilon = 0{\cdot}1$. The $\lambda_i^{(0)}$ are calculated from classical plate theory, and the unperturbed mode shapes are normalized with respect to $M^{(0)}$. With appropriate values substituted in equations (7) and (8), the A_k and B_k are calculated, and the perturbed mode shapes (5) and (6) are normalized to unit peak amplitude. The figures depict circumferential vairation of the transverse displacement at $r = 1$ for each doublet member, and the corresponding Fourier content. In Figure 2, for instance, the $n = 4$ coefficients for S and C have the same numerical value (0·62) as for the normalized modes of the axisymmetric disk. While analogous to a classical four nodal diameter mode, the S and C members of $P(0, 4)$ suffer contamination at harmonics $k = 1, 6, 9, \ldots$, with their distorted appearance depicted in Figure 2(a). With respect to the wavenumber spectrum shown in Figure 2(b), since $k = 9 \in \mathscr{M}$, those coefficients have the same sign and magnitude ($-0{\cdot}08$) as given by equation (7). However, since $k = 1$ and 6 each lie in $\mathscr{P}$, $A_k^{(R)} = -B_k^{(R)}$ at $\pm 0{\cdot}21$ and $\pm 0{\cdot}13$, respectively, for those wavenumbers in equation (8). Likewise, with $n = 6$ in Figure 3 for the $P(0, 6)$ mode, $A_k^{(R)} = B_k^{(R)}$ for $k = 1 \in \mathscr{M}$, but $A_k^{(R)} = -B_k^{(R)}$ for $k = 4$ and 9.

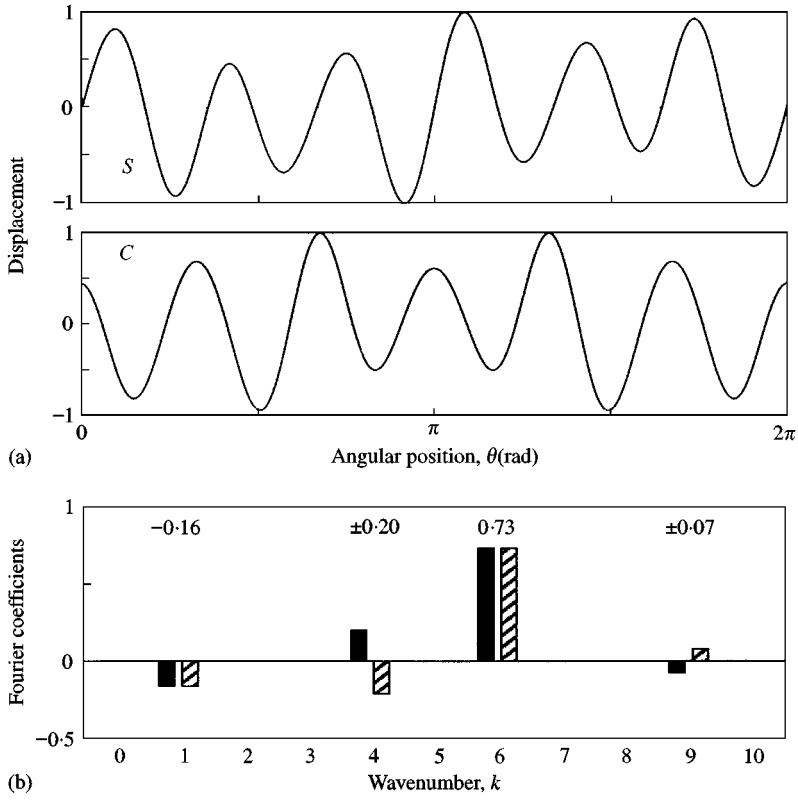

Figure 3. (a) Transverse displacements $U_{06S}^{(R)}$ and $U_{06C}^{(R)}$ at $r = 1$ of the $P(0, 6)$ doublet, and (b) Fourier coefficients R_{06}, $\varepsilon A_k^{(R)}$, ▨, and $\varepsilon B_k^{(R)}$, ■, at $k = 1$, 4 and 9.

2.2. SPLIT DOUBLETS

When $2n = jNF$ ($j = 1, 2, \ldots$), the degenerate frequencies for an axisymmetric structure's doublet generally split. When five features are present, for instance, the frequencies of the 5, 10, 15, … nodal diameter doublets are affected. Conversely, as those features are gradually removed, two frequencies in the periodic structure's spectrum would coalesce. Through the asymptotic analysis, the split doublet eigenvalues of the system in Figure 1 become in the first approximation

$$\lambda_{c,s} \approx \lambda_{c,s}^{(0)} + \varepsilon\lambda_{c,s}^{(1)} = \lambda_{c,s}^{(0)} + \varepsilon \frac{\alpha NF}{2} (k_0 - \lambda_{c,s}^{(0)} m_0) R_{mn}^2(r_0) \left(1 \pm \frac{\sin(n\alpha)}{n\alpha}\right), \tag{10}$$

where $\sqrt{\lambda_c}\,(+)$ and $\sqrt{\lambda_s}\,(-)$ are the dimensionless natural frequencies of the cosine and sine members.

The quality

$$\Delta\lambda = \frac{\lambda_{c,s}^{(1)}}{(k_0 - \lambda_{c,s}^{(0)} m_0) R_{mn}^2(r_0)} \tag{11}$$

is the normalized first-order correction. In the present case, the otherwise split frequencies repeat again whenever $\sin(n\alpha) = 0$, namely, $\alpha = j\pi/n$ ($j = 1, 2, \ldots$). Figure 4 depicts this

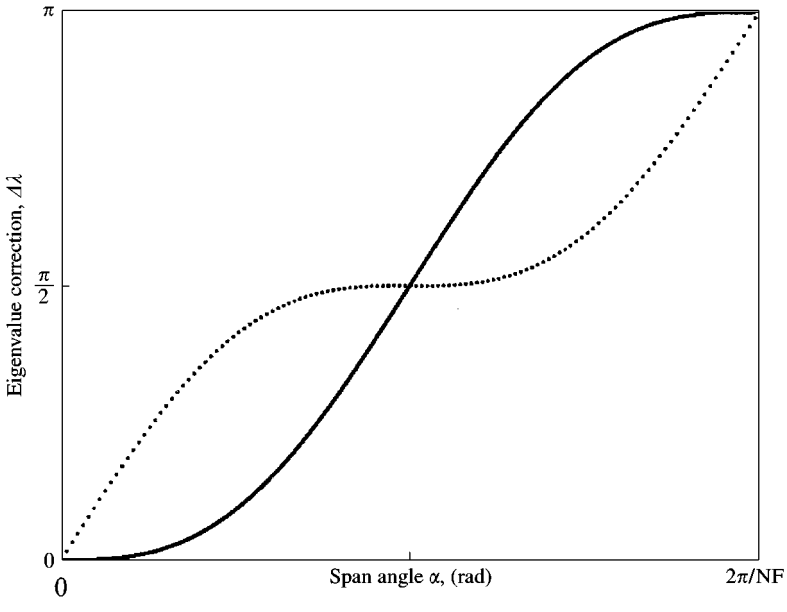

Figure 4. First order eigenvalue corrections for the split sine (——) and cosine (· · ·) doublet members as functions of the span angle α; $NF = 5$ and $n = 5$. The nominally "split" frequencies repeat at $\alpha = \pi/5$.

dependence of $\lambda_{c,s}$ on the span angle for the case $NF = n = 5$. For parameter values as in Figures 2 and 3, C has higher frequency than S for small α, but as the span is increased, the loci cross at $\alpha = \pi/5$. In fact, for larger α, the sine mode's natural frequency is greater than that of the cosine mode. In this light, it is possible for a periodic structure's doublet, which would be expected to split in frequency on the basis of the $2n = jNF$ criterion, to retain repeated frequencies, at least to first order.

With $NF = 5$, for instance, because α lies in $(0, 2\pi/5)$, the frequency loci of the $P(0, 5)SC$ doublet in Figure 4 exhibit only one crossing at $\alpha = \pi/5$. In the same structure, however, the loci for $P(0, 10)SC$ doublet have three crossings at $\alpha = \pi/10$, $\pi/5$ and $3\pi/10$. When NF is odd, the loci of the lowest-frequency split doublet cross only at $\alpha = \pi/NF$, but when NF is even, no such crossing occurs since $n = NF/2$. For instance, $P(0, 3)SC$ is the lowest-frequency split doublet in a structure with six features, but because $0 \leqslant \alpha \leqslant \pi/3$, no frequency crossing point occurs as α is varied.

The eigenfunctions of the doublet become

$$U^{(S)}_{mnc} = R_{mn}(r)\cos(n\theta) + \varepsilon \sum_{k \in \mathscr{K}} A^{(S)}_k(r)\cos(k\theta), \tag{12}$$

$$U^{(S)}_{mns} = R_{mn}(r)\sin(n\theta), \tag{13}$$

where the superscript indicates that the doublet is nominally split. While the sine mode is unaltered to first order, namely $B^{(S)}_k(r) = 0$, the contamination coefficients for the cosine member are

$$A^{(S)}_k(r) = \left(\frac{4n}{NF}\right) C_{mnk}(r)\sin(n\alpha). \tag{14}$$

Notably, the $A_k^{(S)}$ precisely vanish at the crossing points of the eigenvalue loci. At those particular α, the natural frequencies of the "split" doublet repeat, and the mode shapes are identical to first order with those of the axisymmetric disk. For the split doublets, the extent of modulation grows with n, but is inversely proportional to NF.

3. TRAVELLING WAVE RESPONSE

The steady-state near-resonant response of repeated and split doublets when they are subjected to a harmonic travelling wave excitation is discussed in this section. The vibration modes are expressed in the forms (5) and (6) for a repeated doublet, and equations (12) and (13) for a split doublet. In that sense, the structure under consideration can be more general than the model system of Figure 1, to the extent that its doublets admit such representations. Without having independent sine- and cosine-oriented components at identical or nearly identical frequencies, singlets do not produce travelling wave responses, and they are therefore not considered further.

As sketched in Figure 1, the forcing function has spatial wavenumber N, and is concentrated at the radial position r^*, and rotates relative to the disk. As observed in $\chi^{(0)}$, the excitation is

$$f(r, \theta, t) = \frac{F_0}{r}\,\delta(r - r^*)\cos(N\theta + \omega t), \quad r^* \in (r_i, 1), \tag{15}$$

with frequency $\omega = N\Omega$, where the dimensionless F_0 is the physical forcing amplitude per unit length as scaled by $Eh^3/12a^2(1 - v^2)$. With the eigensolutions obtained from the preceding perturbation analysis and normalized to first order with respect to M, the response is determined through modal analysis.

3.1. REPEATED DOUBLETS

When ω is near the common natural frequency $\omega_{mn}^{(R)}$ of the $P(m, n)$ doublet, and the remaining natural frequencies are well-spaced from ω, the response is approximated by superposition of the doublet's two members according to

$$u_{mn}^{(R)}(r, \theta, t) \approx q_{mnc}^{(R)}(t)\,U_{mnc}^{(R)}(r, \theta) + q_{mns}^{(R)}(t)\,U_{mns}^{(R)}(r, \theta). \tag{16}$$

The generalized coordinates $q_{mnc}^{(R)}$ and $q_{mnc}^{(R)}$ have non-zero values in only two circumstances: when $N = n(P(m, n)$ is driven through the base wavenumber), and when $N = k \in \mathscr{K}$ ($P(m, n)$ is driven through contamination wavenumber). The latter situation is further classified according to whether N lies in the $\mathscr{M}$ or $\mathscr{P}$ subsets.

3.1.1. *Case* $N = n$

The generalized coordinates in equation (16) are given by

$$q_{mnc}^{(R)} = \frac{\pi F_0 R_{mn}(r^*)}{\omega^2 - \omega_{mn}^{(R)^2}}\cos(\omega t), \quad q_{mns}^{(R)} = -\frac{\pi F_0 R_{mn}(r^*)}{\omega^2 - \omega_{mn}^{(R)^2}}\sin(\omega t). \tag{17, 18}$$

Following substitution of equations (5) and (6) and equations (17) and (18) into equation (16), the steady state response becomes

$$u_{mn}^{(R)}(r,\theta,t)=\frac{\pi F_0 R_{mn}(r^*)}{\omega^2-\omega_{mn}^{(R)^2}}\begin{pmatrix} R_{mn}(r)\cos(n\theta+\omega t) \\ +\varepsilon\sum_{k\in\mathscr{M}} A_k^{(R)}(r)\cos(k\theta+\omega t) \\ +\varepsilon\sum_{k\in\mathscr{P}} A_k^{(R)}(r)\cos(k\theta-\omega t)\end{pmatrix}. \tag{19}$$

The motion comprises three classes of harmonic waves:

- The base wave $R_{mn}(r)\cos(n\theta+\omega t)$ derives from the doublet's asymptotic nodal diameter structure. This response component has the same wavenumber as the excitation, and propagates in the same (backward) direction and at the same phase speed relative to the disk, as does f.
- The subset $\mathscr{M}$ of contamination waves, each of which also propagates backward in $\chi^{(0)}$, but with different wavenumbers and phase speeds than the excitation.
- The subset $\mathscr{P}$ of contamination waves, each of which propagates in the direction opposite the excitation, and at different phase speeds and with different wavenumbers than f.

As an example, Figure 5 illustrates the response of the $P(0,4)$ doublet for the structure shown in Figure 1 when $N=4$. The structure's response is animated over one period $T=2\pi/N\Omega$ of excitation at five equally spaced instants, and it is decomposed into its Fourier components at wavenumbers n and $\mathscr{K}$. With $NF=5$, $\mathscr{M}=\{9,14,19,\dots\}$ and $\mathscr{P}=\{1,6,11,\dots\}$ for $P(0,4)$. The $n=4$ and $k=9,14,\dots$ components travel backward with f, whereas the $k=1,6,\dots$ components propagate in the forward direction. The slopes of the arrows in the elements of Figure 5 indicate the propagation speed of each response component.

Vibration measurements of rotating structures are often made at a point fixed either in the structure's or in the excitation's, reference frame. The spectral content of such measurements is also of some practical importance. The response (19) as measured in $\chi^{(0)}$ at particular values of θ and r contains a spectral component only at frequency $N\Omega$. The vibration could alternatively be measured in $\chi^{(1)}$ through the substitution $\theta=\phi-\Omega t$. In that case, then $n=4$ component appears stationary as it travels with the same phase speed as f, but the $\mathscr{M}$ and $\mathscr{P}$ components produce content at frequencies $(N\pm k)\Omega$. Since $|N\pm k|=jNF$ $(j=1,2,\dots)$ by hypothesis, the spectrum measured in $\chi^{(1)}$ includes content at frequencies $NF\times\Omega$, $2NF\times\Omega$, and so forth.

3.1.2. *Case* $N\in\mathscr{M}$

For the case in which the excitation's wavenumber is commensurate with a $k\in\mathscr{M}$, the response is

$$u_{mn}^{(R)}(r,\theta,t)=\frac{\varepsilon\pi F_0 A_N^{(R)}(r^*)}{\omega^2-\omega_{mn}^{(R)^2}}\begin{pmatrix} R_{mn}(r)\cos(n\theta+\omega t) \\ +\varepsilon\sum_{k\in\mathscr{M}} A_k^{(R)}(r)\cos(k\theta+\omega t) \\ +\varepsilon\sum_{k\in\mathscr{P}} A_k^{(R)}(r)\cos(k\theta-\omega t)\end{pmatrix}. \tag{20}$$

In this case, the amplitudes of the generalized forces for $q_{mnc}^{(R)}$ and $q_{mns}^{(R)}$ are determined by $\varepsilon A_N^{(R)}$, rather than by R_{mn} in equation (19). The response is therefore qualitatively similar to that in the case $N=n$, except that the amplitudes differ, being scaled by $\varepsilon A_N^{(R)}(r^*)/R_{mn}(r^*)$. Aside from the factor, the structure's response, Fourier decomposition, and spectral content under point measurements made in $\chi^{(0)}$ and $\chi^{(1)}$ are identical here, with say $N=9$, to that shown in Figure 5.

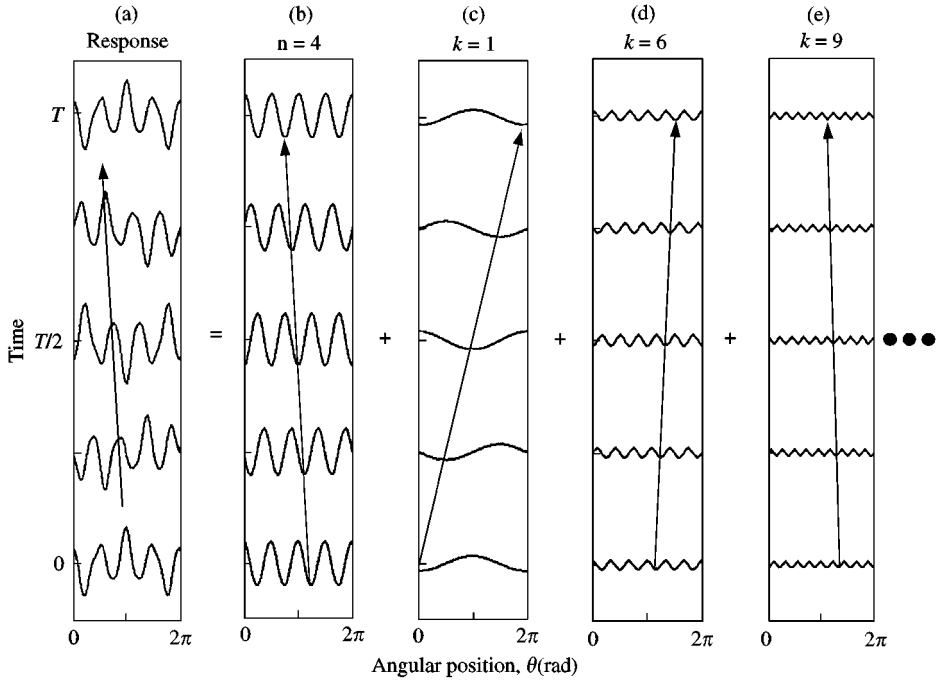

Figure 5. (a) Steady state response in $\chi^{(0)}$ of the $P(0, 4)$ doublet over one excitation period, and its Fourier decomposition (b)–(e); $N = 4$, $NF = 5$, $k_0 = m_0 = 0{\cdot}5$, $\alpha = \pi/10$, and $r_0 = r^* = 1$. Response components with the base $n = 4$ and contamination $k = 9 \in \mathscr{M}$ wavenumbers propagate backward with the excitation, while the contamination $k = 1$ and $6 \in \mathscr{P}$ waves propagate forward. The bold arrow in (a) denotes the direction and rate of the excitation's propagation relative to the disk. Arrows in (b)–(e) indicate the direction and propagation rate for the respective harmonics.

3.1.3. *Case* $N \in \mathscr{P}$

When the excitation's wavenumber lies in $\mathscr{P}$ subset of $\mathscr{K}$, the response is given by

$$u_{mn}^{(R)}(r, \theta, t) = \frac{\varepsilon\pi F_0 A_N^{(R)}(r^*)}{\omega^2 - \omega_{mn}^{(R)^2}} \begin{pmatrix} R_{mn}(r)\cos(n\theta - \omega t) \\ + \varepsilon \sum_{k \in \mathscr{M}} A_k^{(R)}(r)\cos(k\theta - \omega t) \\ + \varepsilon \sum_{k \in \mathscr{P}} A_k^{(R)}(r)\cos(k\theta + \omega t) \end{pmatrix}. \tag{21}$$

Only those response components having wavenumbers in $\mathscr{P}$ travel backward with f; conversely, those components at n and in $\mathscr{M}$ propagate forward. The responses of the $P(0, 4)$ and $P(0, 6)$ doublets, and decompositions into their various wavenumber components, are depicted in Figures 6 and 7.

3.2. SPLIT DOUBLETS

When they are driven by a travelling wave, the members of split doublets superpose in a manner similar to that of the repeated frequency doublets, except that the dynamic magnification factors for the S and C members differ, since generally $\omega_{mnc}^{(S)} \neq \omega_{mns}^{(S)}$. When $N = n$ and ω is near the close but separate natural frequencies, the response in $\chi^{(0)}$ is

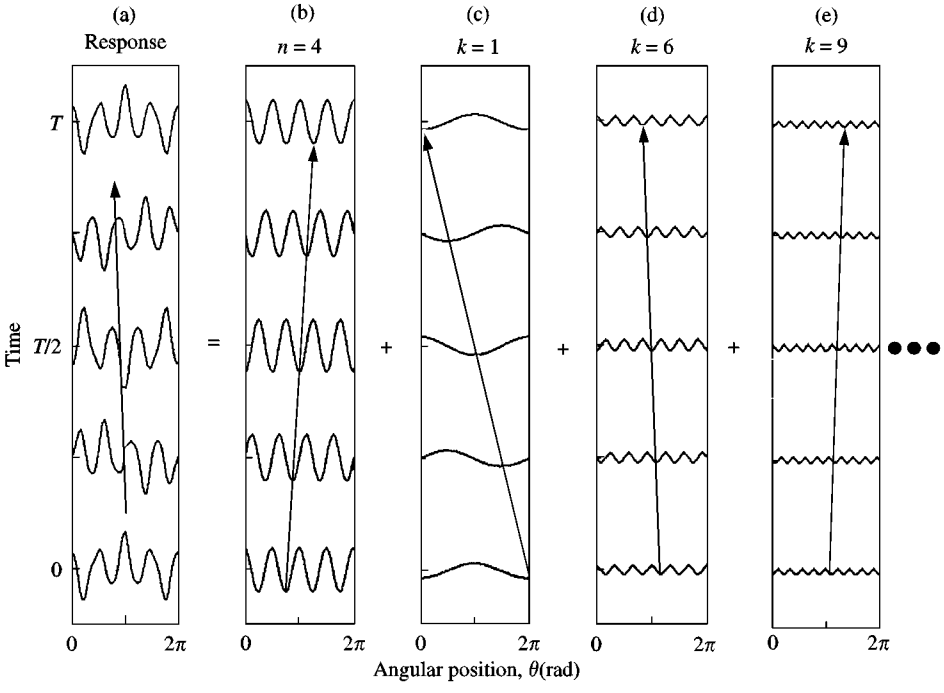

Figure 6. (a) Steady state response in $\chi^{(0)}$ of the $P(0, 4)$ doublet over one excitation period, and its Fourier decomposition (b)–(e); $N = 6$, $NF = 5$, $k_0 = m_0 = 0{\cdot}5$, $\alpha = \pi/10$, and $r_0 = r^* = 1$. Response components with the base $n = 4$ and contamination $k = 9 \in \mathscr{M}$ wavenumbers propagate forward, while the contamination $k = 1$ and $6 \in \mathscr{P}$ waves propagate backward with the excitation. The bold arrow in (a) denotes the direction and rate of the excitation's propagation relative to the disk. Arrows in (b)–(e) indicate the direction and propagation rate for the respective harmonics.

approximately

$$u_{mn}^{(S)}(r, \theta, t) = \pi F_0 R_{mn}(r^*) \begin{pmatrix} R_{mn}(r)\cos(n\theta)\cos(\omega t)/(\omega^2 - \omega_{mnc}^{(S)^2}) \\ - R_{mn}(r)\sin(n\theta)\sin(\omega t)/(\omega^2 - \omega_{mns}^{(S)^2}) \\ + \varepsilon \sum_{k \in \mathscr{K}} A_k^{(S)}(r)\cos(k\theta)\cos(\omega t)/(\omega^2 - \omega_{mnc}^{(S)^2}) \end{pmatrix}, \tag{22}$$

where equations (12) and (13) have been used. In the limit of axisymmetry, the first two terms of equation (22) combine to produce a backward travelling response wave since $\omega_{mnc}^{(S)} = \omega_{mns}^{(S)}$. However, because those frequencies are nominally distinct for $\varepsilon \neq 0$, superposition of the first two components generally produces a combination of travelling and standing wave responses at wavenumber n. The precise balance between those two components depends on ω and its magnitude when compared with $\omega_{mnc}^{(S)}$ and $\omega_{mns}^{(S)}$, as calculated through substitutions in equation (22) of certain trigonometric identities.

The third term appearing in equation (22) is interpreted as the response contributions associated with modulation in $U_{mnc}^{(S)}$, which for each k, appear in $\chi^{(0)}$ as a series of standing waves. When $\omega \approx \omega_{mns}^{(S)}$, the response is dominated by a sine-oriented standing wave at wavenumber n. Likewise, when $\omega \approx \omega_{mnc}^{(S)}$, the response is set primarily by cosine-oriented standing waves having wavenumbers n and each $k \in \mathscr{K}$. To the extent that $R_{mn}(r) > \varepsilon A_k^{(S)}(r)$, the magnitude of the travelling wave component at n will often be greater than that of each standing wave component, at least for excitation frequencies near the intermediate value $\omega_0 = (\omega_{mnc}^{(S)} + \omega_{mns}^{(S)})/2$.

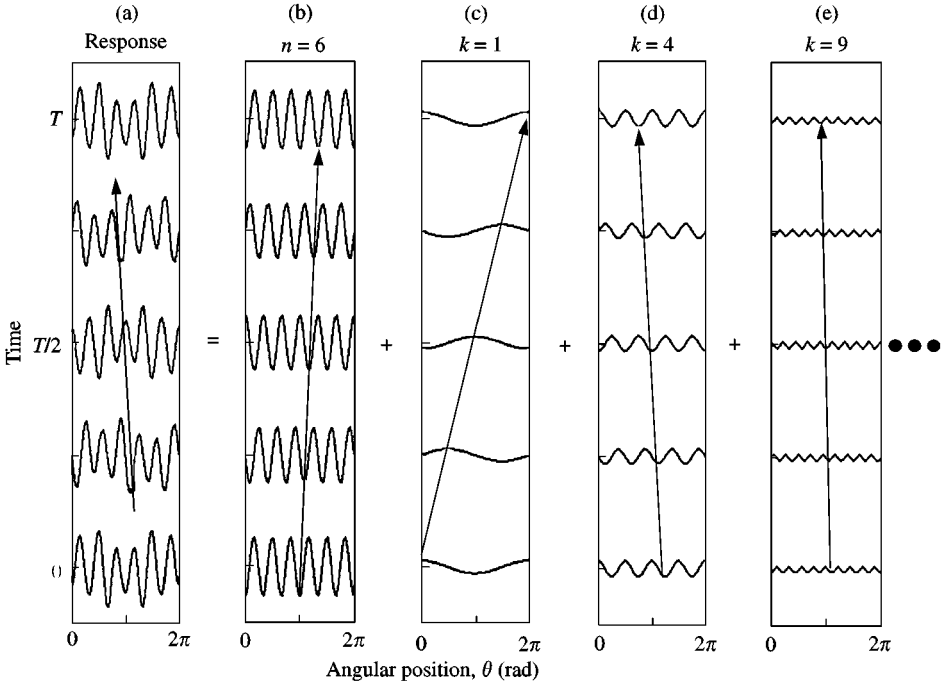

Figure 7. (a) Steady state response in $\chi^{(0)}$ of the $P(0, 6)$ doublet over one excitation period, and its Fourier decomposition (b)–(e); $N = 4$, $NF = 5$, $k_0 = m_0 = 0{\cdot}5$, $\alpha = \pi/10$, and $r_0 = r^* = 1$. Response components with the base $n = 6$ and contamination $k = 1 \in \mathscr{M}$ wavenumbers propagate forward, while the contamination $k = 4$ and $9 \in \mathscr{P}$ waves propagate backward with the excitation. The bold arrow in (a) denotes the direction and rate of the excitation's propagation relative to the disk. Arrows in (b)–(e) indicate the direction and propagation rate for the respective harmonics.

When the nominally split natural frequencies coalesce at $\alpha = j\pi/n$ ($j = 1, 2, \ldots$), each $A_k^{(S)}(r)$ vanishes, and $B_k^{(S)}(r) = 0$ in any case. At that condition, the doublet responds to first order in a manner analogous to that for a repeated doublet of an axisymmetric structure, with resonance at the shifted frequency (10) and only when $N = n$.

For the model structure with parameter values as in Figures 5–7, Figure 8 depicts the norm of the response spectrum of the $P(0, 5)SC$ doublet when excited at $N = 5$, where $|u_{mn}^{(S)}|^2 = \int_0^{2\pi/\omega} \int_0^{2\pi} u_{mn}^{(S)^2}(r^*, \theta, t)\, \mathrm{d}\theta\, \mathrm{d}t$. A travelling wave dominates the response when ω is far from $\omega_{05c}^{(S)}$ and $\omega_{05s}^{(S)}$ to the extent that $R_{mn}(r)$ is substantially greater than each $\varepsilon A_k^{(S)}(r)$, standing waves dominate near either $\omega_{05c}^{(S)}$ and $\omega_{05s}^{(S)}$, and a blend, generally dominated by the travelling wave, exists near ω_0. Qualitative demarcation points between the various regimes are also indicated in the figure.

Finally, when N is instead commensurate with one of the contamination wavenumbers, the response becomes

$$u_{mn}^{(S)}(r, \theta, t) = \frac{\varepsilon\pi F_0 A_N^{(S)}(r^*)}{\omega^2 - \omega_{mnc}^{(S)^2}} \left(R_{mn}(r)\cos(n\theta) + \varepsilon \sum_{k \in \mathscr{K}} A_k^{(S)}(r)\cos(k\theta) \right) \cos(\omega t). \tag{23}$$

In this case, the structure responds in $\chi^{(0)}$ with a linear combination of cosine-oriented standing waves having common frequency but different wavenumbers.

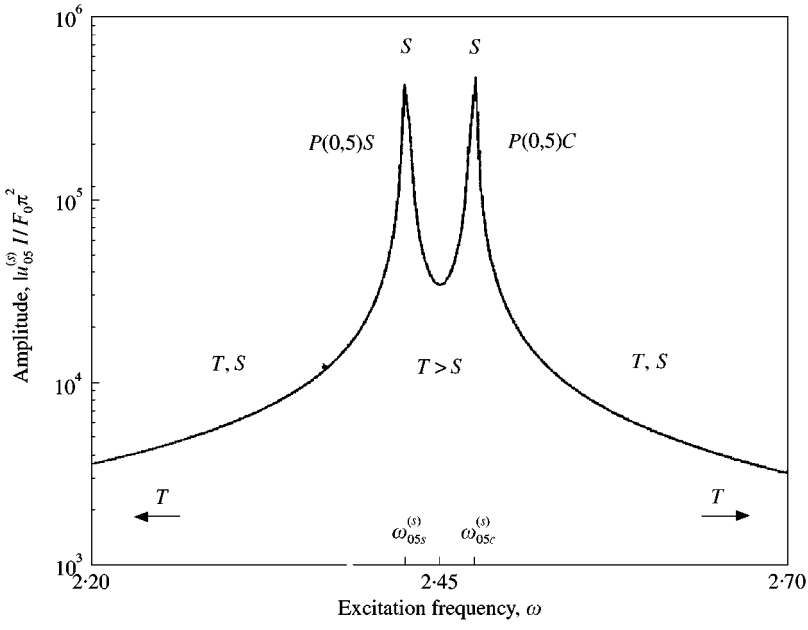

Figure 8. Response amplitude of the $P(0, 5)SC$ doublet, the first order; $N = 5$ ad $r_0 = r^* = 1$. The labels denote regions where the response is dominated by travelling or standing wave components.

4. SUMMARY

The frequency and mode structure of a model rotationally periodic structure, and its forced response when subjected to harmonic travelling wave excitation, are discussed by using a hybrid perturbation and modal analysis approach. Particular emphasis on the behaviour of the repeated and split frequency doublets, which shift in frequency and in wavenumber composition as periodic features are incorporated into an otherwise axisymmetric structural model.

The contamination wavenumbers $k \in \mathscr{K}$ appearing in a repeated doublet are determined through the criterion $|n \pm k| = NF, 2NF, \ldots$, and those wavenumbers are preferentially further classified into subsets $\mathscr{M}$ and $\mathscr{P}$. The Fourier sine and cosine coefficients which define the doublet's modulated shapes are shown to have the same sign when $k \in \mathscr{M}$, but opposite signs when $k \in \mathscr{P}$. That distinction establishes an underlying structure for the doublets which influences both the quantitative and qualitative character of the response under travelling wave excitation. The individual Fourier components comprising a modulated doublet can propagate in the same direction as the excitation or opposite to it, and at the same or different phase speed, depending on the wavenumber of excitation and the subset to which the contamination wavenumber being considered belongs.

ACKNOWLEDGMENTS

This work was supported in part by the National Science Foundation and by AlliedSignal Incorporated, Aerospace Division.

REFERENCES

1. M. KIM, J. MOON and J. A. WICKERT 2000 *American Society of Mechanical Engineers Journal of Vibration and Acoustics* **122**, 62–68. Spatial modulation of repeated vibration modes in rotationally periodic structures.
2. D. L. THOMAS 1974 *Journal of Sound and Vibration* **37**, 288–290. Standing waves in rotationally periodic structures.
3. D. L. THOMAS 1979 *International Journal for Numerical Methods in Engineering* **14**, 81–102. Dynamics of rotationally periodic structures.
4. D. ALLAEI, W. SOEDEL and T. Y. YANG 1987 *Journal of Sound and Vibration* **121**, 547–561. Eigenvalues of rings with radial spring attachments.
5. C. H. J. FOX 1990 *Journal of Sound and Vibration* **142**, 227–243. A simple theory for the analysis and correction of frequency splitting in slightly imperfect rings.
6. I. Y. SHEN and C. D. MOTE 1992 *Journal of Sound and Vibration* **155**, 443–465. Dynamic analysis of finite linear elastic solids containing small elastic imperfections: theory with application to asymmetric circular plates.
7. I. Y. SHEN 1994 *Journal of Sound and Vibration* **172**, 459–470. Vibration of rotationally periodic structures.
8. J.-G. TSENG and J. A. WICKERT 1994 *American Society of Mechanical Engineers, Journal of Vibration and Acoustics* **116**, 468–473. On the vibration of bolted plate and flange assemblies.
9. R. G. PARKER and C. D. MOTE 1996 *American Society of Mechanical Engineers, Journal of Vibration and Acoustics* **118**, 436–445. Exact perturbation for the vibration of almost annular or circular plates.
10. D. J. EWINS and M. IMREGUN 1984 *American Society of Mechanical Engineers, Journal of Vibration and Acoustics, Stress, and Reliability in Design* **106**, 175–180. Vibration modes of packeted bladed disks.
11. T. TOMIOKA, Y. KOBAYASHI, and G. YAMADA 1996 *Journal of Sound and Vibration* **191**, 53–73. Analysis of free vibration of rotating disk-blade coupled systems by using artificial springs and orthogonal polynomials.
12. S. A. TOBIAS and R. N. ARNOLD 1957 *Proceedings of the Institute for Mechanical Engineers*, 669–690. The influence of dynamical imperfection on the vibration of rotating disks.
13. S. C. HUANG and W. SOEDEL 1987 *Journal of Sound and Vibration* **118**, 253–270. Response of rotating rings to harmonic and periodic loading and comparison with the inverted problem.
14. Y. HONDA, H. MATSUHISA and S. SATO 1985 *Journal of Sound and Vibration* **102**, 457–472. Modal response of a disk to a moving concentrated harmonic force..
15. A. PHYLACTOPOULOS and G. G. ADAMS 1995 *Journal of Sound and Vibration* **182**, 415–426. The response of a non-uniformly tensioned circular string to a moving load.
16. W. CAMPBELL 1924 *Transaction of American Society of Mechanical Engineers* **46**, 31–160. The protection of steam-turbine disk wheels from axial vibration.
17. D. J. EWINS 1969 *Journal of Sound and Vibration* **9**, 65–79. The effects of detuning upon the forced vibrations of bladed disks.
18. J. WILDHEIM 1981 *Journal of Sound and Vibration* **75**, 397–416. Excitation or rotating circumferentially periodic structures.
19. W. A. STANGE and J. C. MACBAIN 1983 *American Society of Mechanical Engineers Journal of Vibration, Acoustics, Stress, and Reliability in Design* **105**, 402–407. An investigation of dual mode phenomena in a mistuned bladed disk.
20. R. L. JAY, J. C. MACBAIN, and D. W. BURNS 1984 *American Society of Mechanical Engineers Journal of Engineering for Gas Turbines and Power* **106**, 50–56. Structural response due to blade vane interaction.
21. R. COURANT and D. HILBERT 1953 *Methods of Mathematical Physics*, Vol. 1, 343–350. New York: Wiley.